Spatiotemporal Manipulation of the Mismatch Repair System of Pseudomonas putida Accelerates Phenotype Emergence

Fernández-Cabezón, Lorena; Cros, Antonin; Nikel, Pablo I.

Published in:
ACS Synthetic Biology

Link to article, DOI:
10.1021/acssynbio.1c00031

Publication date:
2021

Document Version
Peer reviewed version

Spatiotemporal manipulation of the mismatch repair system of *Pseudomonas putida* accelerates phenotype emergence

Journal:	*ACS Synthetic Biology*
Manuscript ID	sb-2021-00031q.R1
Manuscript Type:	Article
Date Submitted by the Author:	23-Mar-2021
Complete List of Authors:	Fernández-Cabezón, Lorena; The Novo Nordisk Foundation Center for Biosustainability, Technical University of Denmark Cros, Antonin; The Novo Nordisk Foundation Center for Biosustainability, Technical University of Denmark Nikel, Pablo Ivan; The Novo Nordisk Foundation Center for Biosustainability, Technical University of Denmark

Spatiotemporal manipulation of the mismatch repair system of *Pseudomonas putida* accelerates phenotype emergence

Lorena Fernández-Cabezón, Antonin Cros and Pablo I. Nikel*

The Novo Nordisk Foundation Center for Biosustainability, Technical University of Denmark, 2800 Kongens Lyngby, Denmark

Keywords: *Pseudomonas putida*; Mismatch repair system; Mutagenesis; Synthetic biology; Metabolic engineering; Evolution

Running title: Synthetic mutator devices for phenotype evolution

* Correspondence to: *Pablo I. Nikel* (pabnik@biosustain.dtu.dk)
The Novo Nordisk Foundation Center for Biosustainability,
Technical University of Denmark
Lyngby, Denmark
Tel: (+45 93) 51 19 18

Revision submitted on March 23rd, 2021.

ABSTRACT

Developing complex phenotypes in industrially-relevant bacteria is a major goal of metabolic engineering, which encompasses the implementation of both rational and random approaches. In the latter case, several tools have been developed towards increasing mutation frequencies—yet the precise control of mutagenesis processes in cell factories continues to represent a significant technical challenge. *Pseudomonas* species are endowed with one of the most efficient DNA mismatch repair (MMR) systems found in the bacterial domain. Here, we investigated if the endogenous MMR system could be manipulated as a general strategy to artificially alter mutation rates in *Pseudomonas* species. To bestow a conditional mutator phenotype in the platform bacterium *Pseudomonas putida*, we constructed inducible mutator devices to modulate the expression of the dominant-negative *mutL*^{E36K} allele. Regulatable overexpression of *mutL*^{E36K} in a broad-host-range, easy-to-cure plasmid format resulted in a transitory inhibition of the MMR machinery, leading to a significant increase (up to 438-fold) in DNA mutation frequencies and a heritable fixation of mutations in the genome. Following such accelerated mutagenesis-followed-by selection approach, three phenotypes were successfully evolved: resistance to antibiotics streptomycin and rifampicin (either individually or combined) and reversion of a synthetic uracil auxotrophy. Thus, these mutator devices could be applied to accelerate evolution of metabolic pathways in long-term evolutionary experiments, alternating cycles of (inducible) mutagenesis coupled to selection schemes towards the desired phenotype(s).

INTRODUCTION

Systems metabolic engineering and synthetic biology are used to guide the development of microbial cell factories (MCFs) capable of converting renewable raw materials into value-added compounds[1-3]. However, low productivities and product yields by most MCFs, even after comprehensive optimization of biosynthetic pathways, continue to make the implementation of economically-viable bioprocesses difficult—especially at an industrial scale[4]. Low product yields are often caused by a decrease in cell viability and genetic instability of MCFs under industrially-relevant production conditions[5-6]. For instance, the presence of growth inhibitors in renewable raw materials (e.g. crude glycerol and biomass hydrolysates) and the accumulation of toxic compounds during fermentation (including metabolic intermediates and target products) are known to negatively impact cell survival[7-9].

Adaptive laboratory evolution (ALE), also known as *evolutionary engineering*, is a valuable tool to improve complex phenotypic traits that can be coupled with microbial growth (e.g. tolerance to inhibitors, substrate utilization and growth temperature)[10-12]. At its core, ALE involves the extended propagation of a microbial strain or population, typically over hundreds of generations, in the presence of a desired selective pressure. Mutants that accumulate beneficial mutations will occasionally emerge and expand within the population over time. Selected mutants displaying enhanced phenotypes can be subsequently characterized and sequenced towards reverse engineering[10-15]. Unlike purely rational approaches, ALE facilitates the identification of non-intuitive beneficial mutations that occur in a variety of genes in parallel without requiring any knowledge of underlying genetic mechanisms.

Since intrinsic DNA mutation rates are typically very low (ranging in the order of 10^{-9}–10^{-10} per base pair per generation)[16-17], small and transient increases in mutation frequency can significantly improve the accumulation of beneficial mutations in microbial populations[12,18]. This rationale has been applied to certain ALE experiments, where the genetic diversity of a microbial population was increased before and/or during growth under restrictive culture conditions[5,15,19-20]. Chemical and/or physical mutagenesis techniques have been traditionally used due to their simplicity and wide applicability[21-22], but other genome-wide random mutagenesis techniques can be also applied for this purpose[5]. Mutator strains, i.e. bacteria displaying higher mutation rates, frequently have mutations in one or several genes encoding DNA repair or error-avoidance systems[23]. Most bacteria control DNA substitution rates through

overlapping DNA repair mechanisms, subdivided into three main categories: (i) base selection, (ii) proofreading and (iii) mismatch repair (MMR)[24]. Base selection encompasses the discrimination between correct and incorrect nucleotides by DNA polymerase, while proofreading is the subsequent editing of the newly incorporated nucleotide by a 3'→5' exonuclease activity that hydrolyzes incorrect bases. Following replication, newly replicated DNA is checked by a MMR system that recognizes and corrects mismatches resulting from replication errors[24]. Specific mutations in components of MMR (e.g. *mutL* and *mutS*) or in proofreading DNA polymerases (e.g. *dnaQ*), as well as the overexpression of certain dominant-negative mutator alleles of the same genes, have been shown to result in mutator phenotypes[23,25]. Conditional mutator phenotypes have been applied to the phenotypic optimization of MCFs[26-32]. However, a major problem of these conditional phenotypes is the relatively low control of temporal activity afforded by the cognate devices. A typical drawback of these systems is that the ability of effectively halting DNA mutagenesis is limited, and the cells will continue to mutate even after a desired phenotype is achieved[33].

Pseudomonas putida is a ubiquitous Gram-negative bacterium used for biotechnological and bioremediation applications[34-37]. Strain KT2440, for instance, is a promising microbial *chassis* for handling the synthesis of difficult-to-produce chemicals involving harsh reactions and complex biochemistries[36-40]. Alas, metabolic engineering of *P. putida* still relies largely on trial-and-error approaches. While advanced genome-wide engineering tools are being constantly developed and optimized[41-44], complex phenotypes are the result of multi-level regulatory layers that are often difficult to design from first principles. ALE has recently started to be exploited in *P. putida*-based MCFs[45-50]. On this background, we set out to explore if genome-wide mutation rates in *P. putida* (both wild-type strain and reduced-genome derivatives thereof) could be increased by synthetic control of the well-characterized MMR in this bacterium[51]. To this end, in this work we have designed a toolbox to conditionally increase DNA mutation rates by specifically interfering with the endogenous MMR system towards accelerating the evolution of specific phenotypes. Moreover, we focused on the adoption of emerging strategies to easily cure plasmid-born mutator devices from bacterial populations, such that the temporal window of increased mutagenesis rates can be externally controlled. The application of this set of synthetic mutator devices has been systematically validated in evolution experiments targeting both antibiotic resistance and growth phenotypes *via* reversion of a synthetic auxotrophy.

RESULTS AND DISCUSSION

Construction of broad-host-range, plasmid-based mutator devices to increase DNA mutation rates. *Pseudomonas* species have been shown to display one of the highest MMR efficiencies found in bacteria (e.g. as observed in *P. fluorescens*[52]). Therefore, we hypothesized that manipulating the endogenous MMR system could be a straightforward approach to increase DNA mutation rates in bacterial species of the *Pseudomonas* genus. In order to bestow a conditional mutator phenotype in our model bacterium *P. putida*, we constructed two inducible mutator devices, based on well-characterized expression systems, to tightly modulate the expression of the mutator allele $mutL^{E36K}$ from *P. putida*[51] (**Fig. 1** and **Fig. S1** in the Supporting Information). The E36K amino acid change in MutL stems from a 106(G→A) point mutation in the corresponding allele (**Fig. S1**). The overexpression of the homologous, dominant-negative allele $mutL^{E32K}$ from *Escherichia coli* has been shown to result in a transitory inhibition of the MMR machinery[25,53], which leads to the heritable fixation of mutations in the genome by tampering with the MMR system (**Fig. 1a**). The $mutL^{E36K}$ allele, in contrast, has been exploited for genome engineering approaches specifically developed for *P. putida* and related species[54]. In our mutator devices, the expression of $mutL^{E36K}$ is driven from two tightly-regulated expression systems, i.e. the thermoinducible *c*I857/P_L expression system from bacteriophage λ and the cyclohexanone-inducible ChnR/P_{chnB} system from *Acinetobacter johnsonii*. Both expression vectors have been previously employed for heterologous gene expression in Gram-negative bacteria such as *E. coli* or *P. putida*[55-59]. Thus, the $mutL^{E36K}$ gene was cloned into vectors pSEVA2514 (*c*I857/P_L) and pSEVA2311 (ChnR/P_{chnB}) to yield the mutator plasmids pS2514M and pS2311M, respectively (**Fig. 1b**). The subsequent transfer of the mutator devices and plasmids developed herein to various bacterial hosts is facilitated by adopting the rules set in the *Standard European Vector Architecture* (SEVA) platform[60]. Moreover, the implementation of these two expression systems enables the user to decide whether induction of the devices can be done by a temperature shift (to 40°C) or addition of chemicals to the culture medium (cyclohexanone). These two approaches were selected as the first one (*c*I857/P_L) relies on relieving the transcriptional repression mediated by the *c*I857 protein when it gets degraded at 40°C, whereas the ChnR/P_{chnB} system acts *via* direct activation of the transcriptional response upon addition of a low-cost, small-molecule inducer (**Fig. 1c**). Thermal induction of plasmids pSEVA2514/M was done at 40°C (instead of 42°C, reported to be the most efficient temperature for inactivation of the *c*I857 repressor[61]), because *P. putida* KT2440 can only survive short periods of exposure at 42°C but it can grow for several

hours at 40°C as reported previously[57]. Moreover, thermal induction facilitates alternating cycles of non-induction and induction of DNA mutagenesis by controlling the temperature without the need of removing the inducers from the culture medium—which is oftentimes difficult and time-consuming. The next step was the calibration of these tools as indicated in the sections below.

Emergence of antibiotic resistance phenotypes in *P. putida* carrying synthetic mutator devices. To investigate the functionality of the mutator devices, the occurrence of antibiotic-resistant mutants was assessed in bacterial cultures grown in liquid medium. Two types of antibiotic resistance were selected to this end, namely, rifampicin (Rif) and streptomycin (Str), and the systems were firstly tested in the wild-type strain KT2440. In these experiments, control strains (i.e. *P. putida* KT2440/pSEVA2514 and KT2440/pSEVA2311) and their derivatives carrying the conditional mutator devices (i.e. *P. putida* KT2440/pS2514M and KT2440/pS2311M) were cultured at 30°C in non-selective M9 minimal medium containing 20 mM glucose, and subjected to a mutagenesis protocol as indicated in **Fig. 2** and *Methods*. In the case of strains carrying vectors with the *c*I857/P_L expression system, cultures were shifted at 40°C for 15 min for induction; whereas liquid cyclohexanone was added at 1 mM (and not removed afterwards) in cultures of the strains transformed with vectors bearing the ChnR/P_{chnB} system. Cultures were re-incubated at 30°C and were halted at different phases of bacterial growth (i.e. early-exponential, mid-exponential or stationary phase) to assess the appearance of the target phenotypes.

The occurrence of mutants developing resistance to either Rif or Str was investigated in the bacterial populations after the treatments indicated above. Resistance to these antibiotics has been widely used for the investigation of spontaneous and induced mutagenesis processes in Gram-negative bacteria[62-64]. Rifampicin-resistant (Rif^R) and streptomycin-resistant (Str^R) phenotypes occur due to the appearance of mutations in the *rpoB* and *rpsL* genes, encoding the β-subunit of RNA polymerase and the 30S ribosomal protein S12, respectively[62-65]. Mutation frequencies were estimated by assessing the frequency of occurrence of Rif^R or Str^R cells on the total number of viable cells in the bacterial population for each tested experimental condition (**Fig. 3**). In all accelerated mutagenesis experiments, we observed a significantly higher number of Rif^R and Str^R mutants isolated in selective conditions in bacterial clones carrying a mutator device compared to their respective control strains (**Fig. 3**). A visual example of this general trend is presented in **Fig. S2** in the Supporting Information. The number of Rif^R and Str^R colonies present in 5 mL of non-diluted cultures of *P. putida* KT2440/pSEVA2311 (plated after concentrating the

biomass by centrifugation and resuspension) was roughly similar to that in selective plates seeded with only 100 μL of an undiluted culture of *P. putida* KT2440/pS2311M. When these differences were quantified, we observed that the frequency of appearance of Rif^R and Str^R mutants in *P. putida* KT2440/pS2311M was 438- and 10-fold higher, respectively, as compared to the control strain when the induction of the expression system was stopped in early-exponential growth phase (**Fig. 3a**). In the same experimental conditions, the frequency of occurrence of Rif^R and Str^R mutants in *P. putida* KT2440/pS2514M was 45- and 14-fold higher compared to the control strain, respectively (**Fig. 3b**). Similar relative mutation frequencies were observed when the cultures of the different recombinant strains were prolonged until reaching mid-exponential and stationary phase (**Fig. 3**). The largest differences in mutation frequencies were observed in actively-growing cells (i.e. during the early- or mid-exponential phase of growth) as compared to bacteria harvested during the stationary phase[66-68]. We note that the differences detected in the basal level of mutation frequencies between the two control strains (**Fig. 3**) may be related to intrinsic structural properties of each of the plasmids (e.g. different origins of replication, or the level of expression of regulatory genes therein) and the mutagenesis protocol used (either temperature-shift or addition of a chemical inducer to the culture medium). Although the exact nature of the differences is difficult to quantify, these variables could exert some degree of stress in the host cells[69-70]. Formation of reactive oxygen species, in turn, could lead to a slight increase in the mutation rates[71-72].

Taken together, these experimental data demonstrate the functionality of the mutator devices developed in this work to temporarily increase the global mutation rate in *P. putida*. The differences detected in the mutation frequencies as elicited by the two mutator devices may be related to intrinsic properties of each of the plasmids that carry the mutator allele (e.g. origin of replication and promoter used, since this will affect the transcriptional output), as well as to the protocols followed to induce the expression of $mutL^{E36K}$. Moreover, differences in mutation frequencies are known to arise depending on the method used for their estimation (i.e. counting the occurrence of Rif^R or Str^R clones). On the one hand, mutation frequencies and the actual spectrum of mutations have been shown to vary at different chromosomal positions in several bacterial species, including *P. putida*[73-75]. Other genetic factors, such as the orientation of the target gene in the replication fork, its level of transcription and/or the immediately flanking nucleotides can also influence the mutation frequency[73-74]. On the other hand, the nature of the mutations acquired by *rpoB* (*PP_0447*) and *rpsL* (*PP_0449*) has been demonstrated to lead to distinct levels of resistance to both Rif and Str, which makes it difficult to use these phenotypes for a direct, quantitative estimation of

global mutation rates in different bacterial strains. Factors such as the time and temperature of incubation in selective medium (i.e. agar plates supplemented with antibiotic) have been also shown to dramatically affect the estimation of mutation frequencies (e.g. due to the appearance of colonies with uneven sizes)[64]. Therefore, the utilization of alternative phenotypes is highly recommendable for the calibration and validation of our mutator tool. This issue was undertaken as explained in the next section.

Reversion of a uracil auxotrophy in *P. putida* using mutator devices. To further calibrate the mutator vectors and gain insight into growth phenotypes beyond antibiotic resistance, we investigated the reversion of uracil auxotrophy of the *P. putida pyrF* HM (**Table 1**). This strain is a derivative of reduced-genome *P. putida* EM42 carrying a 163(A→T) mutation in *pyrF*, which results in a Lys55*STOP* change in the PyrF protein[76]. This change, in turn, leads to abortive translation of the cognate mRNA and the strain thus lacks a functional orotidine 5'-phosphate decarboxylase (i.e. Ura$^-$ phenotype), an essential activity for bacterial growth on minimal medium. In these experiments, the control strains, i.e. *P. putida pyrF* HM/pSEVA2514 and *pyrF* HM/pSEVA2311, and the conditional mutator strains, i.e. *P. putida pyrF* HM/pS2514M and *pyrF* HM/pS2311M, were cultured at 30°C in non-selective medium (i.e. with uracil supplementation) and subjected to the mutagenesis protocol indicated in **Fig. 2**. After treatment, the cultures were re-incubated at 30°C, and were harvested upon a doubling in the population size (i.e. early-exponential phase). The emergence of uracil prototrophic mutants (Ura$^+$) in the evolved bacterial populations was determined by seeding M9 minimal medium agar plates with glucose but without uracil supplementation. Mutation frequencies were estimated by assessing the frequency of occurrence of Ura$^+$ mutants on the total number of viable cells in the population for each tested experimental condition (**Fig. 4a**). A significant higher number of Ura$^+$ mutants were isolated from the bacterial populations carrying the conditional mutator devices as compared to their respective control strains, again validating the functionality of the mutator tools. In fact, we only isolated a negligible number (0-4) of spontaneous Ura$^+$ mutants in bacterial populations of control strains under these experimental conditions. Under these conditions, we estimated mutation frequencies with the cyclohexanone-inducible and thermoinducible mutator systems within the same range (i.e. 750 and 860 Ura$^+$ mutants per 1×10^9 viable *P. putida* cells, respectively, **Fig. 4a**). The next objective in this experiment was studying the nature of the mutations acquired by the Ura$^+$ clones.

The conditional mutator phenotype favors the emergence of transition mutations in the genome. To investigate the nature of the mutations introduced with the mutator devices, the whole *pyrF* gene (*PP_1815*) was amplified by high-fidelity PCR from several Ura$^+$ clones and the resulting amplicons were sequenced (**Fig. 4b**). All the revertant (i.e. Ura$^+$) clones had a very similar growth phenotype when grown in M9 minimal medium with glucose as the only carbon source, both when compared to each other or to their parental strain EM42 (**Fig. S3a-d** in the Supporting Information). Firstly, we analyzed and catalogued the mutations that may occur spontaneously at codon 55 of the *pyrF* gene (**Fig. S3e** in the Supporting Information). Next, we isolated multiple Ura$^+$ mutants from two independent evolution experiments performed with the conditional mutator strains (i.e. *P. putida pyrF* HM/pS2514M and *pyrF* HM/pS2311M). The DNA transitions 164(A→G) or 163(T→C), which both eliminate the premature *STOP* codon in the *pyrF*$^{163(A\rightarrow T)}$ variant that leads to uracil auxotrophy, were equally frequent in the mutants analyzed across different independent experiments (**Fig. 4b** and **4c**). These observations indicate that the mutator devices seem to mediate transition mutations, i.e. changes from a purine nucleotide to another purine (i.e. A:T ↔ G:C) or a pyrimidine nucleotide to another pyrimidine (C:G ↔ T:A). Note that only these two transitions could lead to the disappearance of the premature *STOP* codon and to the production of a potentially functional full PyrF protein (**Fig. S3e** in the Supporting Information). When the *pyrF* sequence was analyzed in the few Ura$^+$ mutants isolated from experiments with the controls strains, we found a significant enrichment of transversion mutations, e.g. 163(T→G), 164(A→T) and 164(A→C) (**Fig. 4c**). Interestingly, we could not isolate Ura$^+$ mutants displaying the wild-type *pyrF* sequence (i.e. with a Lys residue at position 55 of PyrF; **Fig. 4b**) in any of these experiments. This finding may be simply due to probabilistic reasons (i.e. number of clones isolated and analyzed, or the topology of the gene and access to the MMR machinery).

In agreement with our results, Long *et al.*[52] showed that transition mutations are 16 to 82-fold more abundant than transversions in bacterial strains lacking a functional MMR system (both *Deinococcus radiodurans* and *P. fluorescens*), in sharp contrast to the mere < 3-fold found in the wild-type strains (i.e. spontaneously occurring). Horst *et al.*[23] also indicated that DNA transitions and frameshift mutations were more abundant in *E. coli* cells lacking a functional MMR system. Regardless of the nature of the mutations introduced by these tools, these experiments show that the conditional mutator devices can be used to accelerate the emergence of different phenotypes. However, a major limitation of this set of plasmid-borne devices is the difficulty of curing them from the target cells, even in the absence of selective

pressure. This shortcoming was fixed by constructing a new generation of 'curable' mutator devices as explained below.

Design and validation of a new generation of plasmid-based, easy-to-cure mutator devices for Gram-negative bacteria. Previous attempts to cure isolated clones from the set of mutator plasmids based on vectors pSEVA2311 and pSEVA2514 proved unsuccessful, even after >10 repeated passages of individual colonies under non-selective conditions (data not shown). This situation not only precludes precise temporal control of the accelerated evolution protocol, but also prevents the precise assessment of the (potential) occurrence of secondary mutations in the genome that do not have a selectable phenotype associated to their emergence. In particular, whole-genome sequencing needs to be performed to study the frequency and nature of mutations arising in conditional mutator strains, as well as the *global* mutation rates—as opposed to the *local* effects in individual genes that confer a macroscopic phenotype. In order to overcome this state of affairs, and due to the tedious work required to cure the mutator and control plasmids in all the strains previously tested, we decided to build a new version of easy-to-cure mutator systems using a technology recently developed in our laboratory. This methodology relies on the target curing of vectors by means of *in vivo* digestion mediated by the I-*Sce*I homing endonuclease[77]. For this purpose, we constructed vectors pS2311SG, pS2514SG, pS2311SGM and pS2514SGM by USER assembly (**Table 1** and **S1**). These standardized vectors, which are all derivatives of pSEVA2311, pSEVA2514, pS2311M and pS2514M, respectively, contain (i) an engineered I-*Sce*I recognition site that can be recognized and cleaved off by the endonuclease I-*Sce*I of *Saccharomyces cerevisiae*[78] and (ii) a module for the constitutive expression of *msfGFP* (i.e. P_{EM7}→*msfGFP*, where the gene encoding the monomeric superfolder GFP is placed under control of the synthetic P_{EM7} promoter) (**Fig. 5a**). This last module facilitates the selection of bacterial clones by examination of green-fluorescent colonies under blue light during the plasmid curing protocol. To this end, the accelerated mutagenesis protocol was upgraded by including a plasmid-curing step (presented in **Fig. S4** in the Supporting Information). In this case, isolated clones are transformed with a helper plasmid that carries the gene encoding the I-*Sce*I endonuclease under control of the 3-methylbenzoate (3-*m*Bz)–inducible XylS/*Pm* expression system. Loss of the plasmid carrying the mutator device can be easily inspected as the corresponding colonies will also lose green fluorescence. Importantly, the presence of mutator plasmids does not affect the growth profile of the host (**Fig. S5** in the Supporting Information).

In these experiments, we firstly subjected the control strains (i.e. *P. putida* KT2440/pS2514SG and KT2440/pS2311SG) and the conditional mutator strains carrying the new set of plasmids (i.e. *P. putida* KT2440/pS2514SGM and KT2440/pS2311SGM) to the standard mutagenesis protocol to confirm the functionality of the easy-to-cure devices (**Fig. S4** in the Supporting Information). We investigated the emergence of Str^R mutants after implementing the accelerated mutagenesis protocol, and new induction conditions were tested to further characterize the tools. As expected, most of the recombinant strains harboring the easy-to-cure plasmids behaved quite similarly to the original strains carrying the first generation mutator devices (**Table S2** in the Supporting Information). The mutation frequency mediated by the mutator allele under control of the *c*I857/P_L expression system was essentially identical in all experiments, irrespective of whether the original or the upgraded set of plasmids was used. We detected a lower mutation frequency in strain KT2440/pS2311SGM (ca. 60% lower than the values observed in strain KT2440/pS2311M under similar experimental conditions). Such a trait was consistently accompanied by loss of green fluorescence in a significant proportion of the bacterial colonies isolated in solid medium, i.e. lysogeny broth (LB) agar, with or without Str supplementation. This result could be due to multiple factors, e.g. accumulation of loss-of-function mutations in the *msfGFP* gene stimulated by the same mutator device or unexpected decay or loss of the mutator plasmid in the absence of selection pressure [i.e. plasmid-borne kanamycin (Km) resistance].

To investigate the hypothesis above, we repeated the accelerated mutagenesis protocol with strain KT2440/pS2311SGM while maintaining Km selection on the plates. We observed that, in the presence of the selection pressure borne by the mutator plasmid, all the bacterial colonies maintained green fluorescence and the overall mutagenesis frequencies were significantly higher than in all previous experiments (e.g. 270-fold higher than in the experiments with the same plasmid but omitting Km; **Table S2**). Under these experimental conditions, the cyclohexanone-inducible mutator plasmids appear to exhibit leaky expression of the *mutL*^{E36K} allele, which led to similar mutagenesis frequencies in the absence or presence of inducer (**Table S2**). This observation helps explaining why, in the absence of selection pressure, some cells may reduce the copy number of the pS2311SGM plasmid to alleviate the mutagenic effects caused by (semi)constitutive expression of *mutL*^{E36K}—or even force complete plasmid loss in some clones. Most of the colonies analyzed in these experiments showed a significant reduction in the plasmid copy number (and not a total loss of plasmid) accompanied by a dramatic reduction in the fluorescence levels. At the bacterial population level, this phenomenon could further translate into an

overall decrease of the *global* mutagenesis frequency. This behavior was not observed in strain KT2440/pS2514SGM, which appears to exhibit a lower—but more tightly-regulated—expression level of the mutator allele than the ChnR/P_{chnB} counterpart (**Table S2**). Actually, extending the thermal induction of the *c*I857/P_L-based mutator devices from 15 to 30 min did not affect the *global* mutagenesis frequency. In either case, the genetic upgrading of the plasmid toolbox was meant to facilitate the easy curing of the mutator devices, and the results of these experiments are explained in the next section.

Easy-to-cure mutator devices enable a tight control of the global mutagenesis and reveal a wide landscape of genome modifications upon accelerated evolution. We decided to sequence the whole genome of several colonies isolated in non-selective medium (i.e. LB agar, 2-5 colonies for each experimental condition) in order to assess the frequency and nature of mutations mediated by the mutator devices. To this end, green-fluorescent colonies were selected after treatment (**Fig. S4** in the Supporting Information) and transformed with the helper pQURE6·L plasmid[77], a conditionally-replicating vector that requires supplementation of 3-*m*Bz to the culture medium to ensure plasmid maintenance (**Fig. S6** in the Supporting Information). As indicated above, plasmid pQURE6·L carries a synthetic module for the 3-*m*Bz–inducible expression of the *I-SceI* endonuclease gene (i.e. XylS/*Pm→I-SceI*; **Table 1**) and a second module for the constitutive expression of *mRFP* (i.e. P_{14g}→*mCherry*), which, together, facilitate quick curing of mutator plasmids by positive selection of red-fluorescent colonies (**Fig. S4** in the Supporting Information; see also *Methods* for details on the curing procedure). In all cases, the mutator devices could be easily cured upon introduction of plasmid pQURE6·L. Moreover, this helper plasmid could be typically cured during a simple overnight incubation of individual colonies in LB medium without 3-*m*Bz (data not shown), similarly to the observations reported by Volke *et al*.[77]

Multiple colonies were isolated from the accelerated mutagenesis experiments using the upgraded mutator toolbox and, upon curing all plasmids, genomic DNA was extracted and purified prior to next generation sequencing. Whole-genome sequencing of genomic DNA enabled a precise elucidation of the nature of mutations elicited by these devices. In general, whole-genome sequencing data confirmed our previous findings, as the emergence of transitions was a clear signature of clones carrying the *mutL*^{E36K} allele in different configurations (**Fig. 5b** and **Table S3** in the Supporting Information). These single-nucleotide polymorphisms were largely non-synonymous, and transversions were observed to be extremely rare (i.e. 1 transversion per genome in a just a few isolated clones, no different from the

frequency of transversions in any of the control strains). Importantly, the mutator devices also promoted the emergence of small insertion-deletion mutations (InDel, mostly consisting of 1-2 bp; **Fig. 5b** and **Table S4** in the Supporting Information). Frameshift insertions were the most abundant type of InDels detected in the isolated clones. Taken together, and consistently with the results of experiments reported in the previous section, the detailed exploration of mutations elicited by the cyclohexanone-inducible mutator devices indicate that this system promotes a nearly-constitutive mutator phenotype. This feature, in turn, triggers a relatively high mutagenesis frequency over short induction periods—probably caused by the leakiness observed for this system under these conditions.

Evolution of dual antibiotic resistances in *P. putida* with mutator devices. The results discussed in the previous sections indicate that the enrichment of point mutations afforded by the conditional mutator systems can be harnessed to select for monogenetic phenotype traits. Next, we asked the question if the system can be used to accelerate the emergence of more complex phenotypes. To this end, we adopted dual resistance to Rif^R and Str^R as a proxy. The upgraded mutagenesis protocol (**Fig. S4**) was repeated by using *P. putida* KT2440 as the host, transformed with either vector pSEVA2311SG (control) or plasmid pS2311SGM (where the mutagenic $mutL^{E36K}$ allele is controlled by a ChnR/P_{chnB} module). After incubating the cultures in M9 minimal medium with 20 mM glucose for 24 h, the emergence of double-resistant mutants was estimated by plating the bacterial suspension onto LB agar supplemented with Km, Rif and Str. As observed in experiments involving single antibiotic resistances, a significant difference in the number of Km^R, Rif^R and Str^R was immediately evident when comparing plates seeded with *P. putida* KT2440/pSEVA2311SG or *P. putida* KT2440/pS2311SGM even by the naked eye (**Fig. 6a**). Indeed, the emergence of double Rif^R and Str^R *P. putida* mutants was 6-folder higher in cultures of cells carrying the mutator device than in control experiments (**Fig. 6b**). These results validate the use of the tools constructed herein for the evolution of multigenic traits by the adoption of a simple protocol that can be iterated (and even automated) as needed.

CONCLUSION

In this work, we have constructed two synthetic biology devices to control the mutation rate in *P. putida*—and, due to the nature of the vectors used for these constructs, other Gram-negative bacteria as well—in a precise spatiotemporal fashion. Transiently overexpressing the endogenous dominant negative

mutL^{E36K} allele of *P. putida* interfered with the normal functioning of the endogenous MMR machinery, thereby increasing mutation frequencies in multiple strains of *P. putida* by 2- to 438-fold. Following a 'mutagenesis-followed-by selection' approach, we have successfully evolved three separate phenotypes arising from monogenic traits, i.e. resistance to the antibiotics Str and Rif and uracil prototrophy. Within this approach, we have firstly increased the genetic diversity in the bacterial population by inducing the activity of the synthetic mutator devices and, subsequently, isolated mutants onto a selective solid medium. In these experiments, the expression of the mutator *mutL*^{E36K} allele was driven from two inducible modules, i.e. the thermoregulated *c*I857/P_L and the cyclohexanone-regulated ChnR/P_{chnB} expression systems, which have been previously tailored for heterologous gene expression in different Gram-negative bacterial species. We observed that the mutation frequencies achieved with the cyclohexanone-inducible mutator devices (i.e. vectors pS2311M and pS2311SGM, which represent the first and second generation of the tools constructed in this study) were significantly higher than those obtained with the thermoinducible mutator counterparts (i.e. vectors pS2514M and pS2514SGM) under most of the experimental conditions tested. In agreement with previous studies conducted with *E. coli* and related species, we have also observed a higher emergence of transition and frameshift (InDel) mutations in cells displaying a temporarily-tampered MMR system[23]. We note, however, that this fact should not be interpreted as an inherent limitation of the mutator devices developed here, since all of the available mutagenesis techniques exhibit mutation biases to different degrees[21,79]. The preferential enrichment of a certain type of mutations is thus unavoidable, irrespective of the system used to induce mutagenesis.

Interestingly, the cyclohexanone-triggered mutator devices had a significant level of leaky expression of *mutL*^{E36K}, which in turn promoted a nearly-constitutive mutator phenotype that lead to high mutagenesis rates. The mutation frequencies achieved with this system were, however, lower than those reported with constitutive mutator strains where the mutator phenotype was originated by modifications in components of the endogenous MMR system. For example, Kurusu *et al*.[80] reported that the frequency of occurrence of Rif^R mutants in a Δ*mutS* derivative of *P. putida* KT2440 was 1,000-fold higher than that in the wild-type strain. Since mutation rates must be precisely controlled to avoid extensive accumulation of deleterious mutations and to prevent genomic instability, the overexpression of mutator alleles should be driven from tightly-regulated expression systems (which is always challenging, irrespective of the bacterial host[59]) or during short periods of time. Thus, the easy-to-cure mutator plasmids developed in this study, which can be rapidly removed from isolated clones displaying the phenotype of interest, offer a clear advantage over

conventional mutator strains—where the mutator phenotype is elicited by genomic (hence, essentially irreversible) modifications, as epitomized by the emergence of mutator phenotypes of *P. aeruginosa* in clinically-relevant setups[81-82]. In contrast with the results of the ChnR/P_{chnB}-dependent module, the thermoinducible mutator devices allowed for a tightly-regulated expression of *mutL*^{E36K}. This tool may be applied to long evolutionary experiments that involves alternating cycles of non-induction and induction of mutagenesis coupled to phenotype selection (e.g. growth-coupled approaches). By modifying the induction conditions and the number of induction cycles, a landscape of mutation rates could be achieved and adapted to the needs of each evolutionary experiment. The control of these parameters might be crucial for accelerating the evolution of complex phenotypes in industrial MCFs, since it has been previously shown that microbial adaptation to specific stresses is favored with certain mutation rates[83]. Due to its particular metabolic architecture, this would likely be the case for *P. putida* as well[84].

Along the same line, the method described herein suppresses the need of handling chemical or physical mutagens—which are typically carcinogenic and, oftentimes, acutely toxic—for phenotype evolution. As an example, implementing physical methods for mutagenesis (e.g. UV irradiation) in liquid cultures is not only technically difficult but will unavoidably result in an uneven exposure of the cells to the irradiation source[85]. UV irradiation results in a single type of mutation in the DNA (i.e. thymine dimer lesions), thereby reducing the mutational landscape that can be obtained with such method. Thus, using mutator plasmids represents an advantage over the adoption of traditional mutagens, enabling safer operation conditions and circumventing the subsequent treatment of contaminated materials. Also, the thermoinducible mutator device described herein allows to alternate cycles of non-induction and induction of mutagenesis by merely controlling the incubation temperature—altogether suppressing the addition of any chemicals to the culture medium.

From a more general perspective, it should be noted that the MutL/MutS protein complex of the MMR machinery appears to be well-conserved in most bacterial species[86-87]. For instance, the MutS protein from *P. putida* and the MutL protein from *P. aeruginosa* were shown to functionally complement Δ*mutS* and Δ*mutL* mutants of *E. coli* and *Bacillus subtilis*, respectively[80,88]. Therefore, the broad-host-range mutator devices developed herein are expected to be functional in other bacterial hosts as well. In addition to their application for the accelerated evolution of phenotypes that depend on multiple mutations across the bacterial genome, the use of these devices also revealed an important feature of the MMR system

relevant for synthetic biology. A number of genome modification approaches rely on specifically interfering with the bacterial MMR system to enable strand invasion[51,53,59,89]. Besides the intended modifications (e.g. as encoded in mutagenic oligonucleotides), there are several secondary mutations that could occur due to overexpression of mutagenic alleles. The tight spatiotemporal manipulation of this trait, afforded by the plasmids reported in this study, could enable a more precise control of genome modifications by restricting the mutation landscape to the intended alterations.

METHODS

Bacterial strains and growth conditions. The bacterial strains used in this work are listed in **Table 1**. *E. coli* DH5α was used for cloning and plasmid maintenance. *E. coli* and *P. putida* strains were routinely grown in lysogeny broth (LB) medium (10 g L^{-1} tryptone, 5 g L^{-1} yeast extract and 5 g L^{-1} NaCl) at 37°C and 30°C, respectively, in an orbital shaker at 150 rpm. For mutagenesis experiments, *P. putida* was grown in M9 minimal medium supplemented with 20 mM glucose as the sole carbon source—as typically done when cultivating this species on sugars for physiological studies[84]. Cyclohexanone was added at 1 mM to cultures for induction of *mutL*^{E36K} expression as necessary. When appropriate, antibiotics were also added at the following concentrations (μg mL^{-1}): gentamicin, 10; Km, 50; Str, 100; and Rif, 50. Supplementation of 20 μg mL^{-1} uracil was implemented to support bacterial growth of uracil-auxotrophic strains. Bacterial growth was estimated by measuring the optical density at 630 nm (OD_{630}).

General DNA manipulations and sequencing. Molecular biology techniques were performed essentially as described in standard protocols[90]. Oligonucleotides were purchased from Integrated DNA Technologies (IDT; Leuven, Belgium) and their sequences are provided in **Table S1** in the Supporting Information. DNA amplification was performed on a C1000 Touch™ Thermal Cycler (Bio-Rad Corp., Hercules, CA, USA) using Phusion *U* Hot Start DNA Polymerase or Phusion Hot Start II DNA Polymerase from Thermo Fisher Scientific (Waltham, MA, USA). DNA fragments were purified with a NucleoSpin™ Gel and PCR Clean-up kit (Macherey-Nagel, Düren, Germany). Restriction enzymes and T4 DNA ligase were obtained from Thermo Fisher Scientific and were used according to the supplier's specifications. USER assembly was performed essentially as described by Nour-Eldin *et al*.[91] with the commercial USER enzyme from New England BioLabs (NEB, Ipswich, MA, USA). Plasmid DNA was prepared with a NucleoSpin™ Plasmid EasyPure kit (Macherey-Nagel). *E. coli* chemical competent cells were prepared

using the *Mix & Go E. coli* Transformation Kit from Zymo Research (Irvine, CA, USA). DNA amplification from a single colony (i.e. colony PCR) was performed with One *Taq* 2× Master Mix (NEB). Electrocompetent *P. putida* cells were prepared by washing twice an overnight culture of *P. putida* with 300 mM sucrose[92]. All cloned inserts and DNA fragments were confirmed by DNA sequencing (Eurofins Genomics, Ebersberg, Germany).

Construction of broad-host range mutator expression vectors. Plasmid pSEVA2514-*rec2-mutL*$_{E36K}^{PP}$, described by Aparicio *et al*.[54], was double-digested with *Xba*I and *Hin*dIII to obtain a 1.9-kb DNA fragment corresponding to the dominant-negative mutator allele *mutL*^{E36K} of *P. putida* KT2440. The purified DNA fragment was subsequently ligated with the pSEVA2541 and pSEVA2311 vectors, previously digested with the same restriction enzymes, to generate plasmids pS2514M and pS2311M, respectively. The easy-to-cure plasmids pS2514SG, pS2514SGM, pS2311SG and pS2311SGM, were subsequently constructed by USER assembly with the primers indicated in **Table S1**. These vectors contain an engineered I-*Sce*I recognition site and an *msfGFP* gene under the control of the constitutive P_{EM7} promoter (**Fig. S4** in the Supporting Information), that make them compatible with the plasmid curation approach recently developed by Volke *et al*.[77].

Accelerated evolution experiments with *P. putida* recombinant strains carrying mutator plasmids. Overnight pre-cultures of the conditional mutator strains [e.g. *P. putida* KT2440/pS2514(SG)M and KT2440/pS2311(SG)M], as well as of their respective control strains [e.g. *P. putida* KT2440/pS2514(SG) and KT2440/pS2311(SG)], were used to inoculate 25 mL of non-selective M9 minimal medium at an initial OD_{600} of 0.075. After 5 h of incubation in an orbital shaker at 30°C (OD_{600} = 0.3), the expression systems were induced thermally (by incubation at 40°C for 15 min in a water bath) or chemically (with addition of 1 mM cyclohexanone). The cultures were subsequently re-incubated at 30°C with shaking and stopped after 1.5 h (early-exponential phase, OD_{600} = 0.6), 2 h (mid-exponential phase, OD_{600} = 1) or 24 h (stationary phase, OD_{600} = 3). Several aliquots of bacterial cultures were plated on selective solid medium (e.g. LB agar supplemented with 100 μg mL^{-1} Str or with 50 μg mL^{-1} Rif as appropriate) to determine the appearance of mutant cells (e.g. Rif^R or Str^R) in the bacterial population. The total number of viable cells in the bacterial population was also estimated by plating dilutions of the cultures on non-selective medium (e.g. LB agar plates). After 32 h of incubation at 30°C, the number of colony forming units (CFUs) in the different culture conditions was estimated by visual inspection of the plates (see **Fig. S2** in the Supporting

Information for an example). At least two biological replicates and two technical replicates were performed for each bacterial strain and selective culture condition, respectively.

Vector curing procedure for easy-to-cure plasmids carrying mutator devices. Overnight pre-cultures of green-fluorescent colonies isolated from evolution experiments were transformed by electroporation with plasmid pQURE6·L (**Table 1** and **Fig. S6**). Transformed cells were recovered in LB medium supplemented with 2 mM 3-*m*Bz during 2 h. Dilutions were then plated on LB agar supplemented with 10 μg mL^{-1} Gm and 1 mM 3-*m*Bz. Red-fluorescent colonies that had lost the mutator plasmids were easily isolated after 24-48 h of incubation at 30°C. For curing the helper pQURE6·L plasmid, overnight pre-cultures of red-fluorescent colonies were grown and dilutions were plated on non-selective medium (e.g. LB agar). Non-fluorescent colonies were selected after 24 h of incubation and were stored for further analysis. Loss of both plasmids in the selected colonies was further confirmed by Gm and Km sensitivity (**Fig. S4**).

Genomic DNA purification, library construction, and whole genome sequencing (WGS). DNA was purified using the PureLink™ Genomic DNA purification kit (Invitrogen, Waltham, MA, USA) from 2 mL of overnight LB cultures inoculated from cryostocks prepared after curing the plasmids from the strains. The genomic DNA of each sample was randomly sheared into short fragments of about 350 bp using ultrasonic interruption. Short and large DNA fragments were removed using magnetic bead size selection and subsequently verified by capillary gel electrophoresis. The obtained DNA fragments were subjected to library construction using the *NEBNext*™ DNA Library Prep Kit (NEB), following the supplier's specifications. Libraries quality control was performed with a Qubit® 2.0 fluorometer and an Agilent™ 2100 BioAnalyzer. Subsequent sequencing was performed using the Illumina NovaSeq™ 6000 PE150 platform. The original sequencing data acquired by high-throughput sequencing platforms recorded in image files were firstly transformed to sequence reads by base calling with the Illumina's CASAVA software. The sequences and corresponding sequencing quality information were stored in a FASTQ file. For quality-control purposes, paired reads were discarded when: (i) either read contains adapter contamination, (ii) uncertain nucleotides (N) constitute >10% of either read, or (iii) low quality nucleotides (base quality less than 5, $Q \leq 5$) constitute >50% of either read. The effective sequencing data were aligned with the reference sequence (NCBI Reference Sequence: NC_002947.4) through Burrows-Wheeler Aligner (BWA) software[93], and the mapping rate and coverage were counted according to the

alignment results. The duplicates were removed by means of the SAMtools package[94]. Single nucleotide polymorphisms (SNPs) and InDels were detected using SAMtools and followed by annotation using ANNOVAR[95]. Libraries construction, sequencing and subsequent data quality control was performed by Novogene Co. Ltd. (Cambridge, United Kingdom).

SUPPORTING INFORMATION

Table S1. Oligonucleotides used in this work.

Table S2. Mutation frequencies estimated with the different versions of mutator plasmids created in this work.

Table S3. Distribution of single nucleotide polymorphisms (SNP) in evolved populations of *P. putida*.

Table S4. Distribution of small insertion-deletion (InDel) mutations in evolved populations of *P. putida*.

Figure S1. Protein sequence alignment of the NH_2-terminal region of MutL proteins from different bacteria.

Figure S2. Appearance of rifampicin- and streptomycin-resistant mutants in populations of *P. putida* KT2440 carrying a mutator device.

Figure S3. Growth profile and characteristics of selected *P. putida* Ura^+ mutants isolated in mutagenesis experiments.

Figure S4. Upgraded protocol for accelerated evolution of phenotypes using the new generation of easy-to-cure mutator devices.

Figure S5. Growth profile of engineered *P. putida* strains carrying mutator plasmids.

Figure S6. Physical map of the helper pQURE6·L plasmid.

AUTHOR CONTRIBUTIONS

L.F.C. and P.I.N. designed the experimental plan and the overall research setup. L.F.C. and A.C. carried the experimental work and drafted the figures and the manuscript, with further contributions by P.I.N. All authors discussed the results and interpreted the experimental data.

ACKNOWLEDGEMENTS

We thank V. de Lorenzo and his team at CNB-CSIC (Madrid, Spain) for sharing research materials and for enlightening discussions. The financial support from The Novo Nordisk Foundation (grants NNF20CC0035580 and *LiFe*, NNF18OC0034818), the Danish Council for Independent Research (*SWEET*, DFF-Research Project 8021-00039B), and the European Union's Horizon 2020 Research and Innovation Programme under grant agreement No. 814418 (*SinFonia*) to P.I.N. is gratefully acknowledged. L.F.C. was supported by the European Union's Horizon 2020 Research and Innovation Programme under the Marie Skłodowska-Curie grants agreements No. 713683 (*COFUNDfellowsDTU*) and No. 839839 (*DONNA*).

CONFLICT OF INTEREST

The authors declare no financial or commercial conflict of interest.

REFERENCES

1. Calero, P., and Nikel, P. I. (2019) Chasing bacterial *chassis* for metabolic engineering: A perspective review from classical to non-traditional microorganisms. *Microb. Biotechnol. 12* (1), 98-124.
2. Chen, Y., Banerjee, D., Mukhopadhyay, A., and Petzold, C. J. (2020) Systems and synthetic biology tools for advanced bioproduction hosts. *Curr. Opin. Biotechnol. 64*, 101-109.
3. Choi, K. R., Jang, W. D., Yang, D., Cho, J. S., Park, D., and Lee, S. Y. (2019) Systems metabolic engineering strategies: Integrating systems and synthetic biology with metabolic engineering. *Trends Biotechnol. 37* (8), 817-837.

4. Ko, Y. S., Kim, J. W., Lee, J. A., Han, T., Kim, G. B., Park, J. E., and Lee, S. Y. (2020) Tools and strategies of systems metabolic engineering for the development of microbial cell factories for chemical production. *Chem. Soc. Rev. 49* (14), 4615-4636.

5. Fernández-Cabezón, L., Cros, A., and Nikel, P. I. (2019) Evolutionary approaches for engineering industrially-relevant phenotypes in bacterial cell factories. *Biotechnol. J. 14* (9), 1800439.

6. Gong, Z., Nielsen, J., and Zhou, Y. J. (2017) Engineering robustness of microbial cell factories. *Biotechnol. J. 12* (10), 1700014.

7. Amoah, J., Kahar, P., Ogino, C., and Kondo, A. (2019) Bioenergy and biorefinery: Feedstock, biotechnological conversion, and products. *Biotechnol. J. 14* (6), e1800494.

8. Poblete-Castro, I., Wittmann, C., and Nikel, P. I. (2020) Biochemistry, genetics, and biotechnology of glycerol utilization in *Pseudomonas* species. *Microb. Biotechnol. 13* (1), 32-53.

9. Becker, J., and Wittmann, C. (2019) A field of dreams: Lignin valorization into chemicals, materials, fuels, and health-care products. *Biotechnol. Adv. 37* (6), 107360.

10. Portnoy, V. A., Bezdan, D., and Zengler, K. (2011) Adaptive laboratory evolution—Harnessing the power of biology for metabolic engineering. *Curr. Opin. Biotechnol. 22* (4), 590-594.

11. Dragosits, M., and Mattanovich, D. (2013) Adaptive laboratory evolution—Principles and applications for biotechnology. *Microb. Cell Fact. 12*, 64.

12. Winkler, J. D., and Kao, K. C. (2014) Recent advances in the evolutionary engineering of industrial biocatalysts. *Genomics 104* (6), 406-411.

13. Shepelin, D., Hansen, A. S. L., Lennen, R. M., Luo, H., and Herrgård, M. J. (2018) Selecting the best: Evolutionary engineering of chemical production in microbes. *Genes 9* (5), 249.

14. Jang, S., Kim, M., Hwang, J., and Jung, G. Y. (2019) Tools and systems for evolutionary engineering of biomolecules and microorganisms. *J. Ind. Microbiol. Biotechnol. 46* (9-10), 1313-1326.

15. Sandberg, T. E., Salazar, M. J., Weng, L. L., Palsson, B. Ø., and Feist, A. M. (2019) The emergence of adaptive laboratory evolution as an efficient tool for biological discovery and industrial biotechnology. *Metab. Eng. 56*, 1-16.

16. Drake, J. W. (1991) A constant rate of spontaneous mutation in DNA-based microbes. *Proc. Natl. Acad. Sci. USA 88* (16), 7160-7164.

17. Lang, G. I., and Murray, A. W. (2008) Estimating the per-base-pair mutation rate in the yeast *Saccharomyces cerevisiae*. *Genetics 178* (1), 67-82.

18. Swings, T., van den Bergh, B., Wuyts, S., Oeyen, E., Voordeckers, K., Verstrepen, K. J., Fauvart, M., Verstraeten, N., and Michiels, J. (2017) Adaptive tuning of mutation rates allows fast response to lethal stress in *Escherichia coli*. *eLife 6*, e22939.

19. Kang, M., Kim, K., Choe, D., Cho, S., Kim, S. C., Palsson, B. Ø., and Cho, B. K. (2019) Inactivation of a mismatch-repair system diversifies genotypic landscape of *Escherichia coli* during adaptive laboratory evolution. *Front. Microbiol. 10*, 1845.

20. Wang, X., Li, Q., Sun, C., Cai, Z., Zheng, X., Guo, X., Ni, X., Zhou, W., Guo, Y., Zheng, P., Chen, N., Sun, J., Li, Y., and Ma, Y. (2019) *GREACE*-assisted adaptive laboratory evolution in endpoint fermentation broth enhances lysine production by *Escherichia coli*. *Microb. Cell Fact. 18* (1), 106.

21. Foster, P. L. (1991) *In vivo* mutagenesis. *Methods Enzymol. 204*, 114-125.

22. Kodym, A., and Afza, R. (2003) Physical and chemical mutagenesis. *Methods Mol. Biol. 236*, 189-204.

23. Horst, J. P., Wu, T. H., and Marinus, M. G. (1999) *Escherichia coli* mutator genes. *Trends Microbiol. 7* (1), 29-36.

24. Schaaper, R. M. (1993) Base selection, proofreading, and mismatch repair during DNA replication in *Escherichia coli*. *J. Biol. Chem. 268* (32), 23762-23765.

25. Aronshtam, A., and Marinus, M. G. (1996) Dominant negative mutator mutations in the *mutL* gene of *Escherichia coli*. *Nucleic Acids Res. 24* (13), 2498-2504.

26. Selifonova, O., Valle, F., and Schellenberger, V. (2001) Rapid evolution of novel traits in microorganisms. *Appl. Environ. Microbiol. 67* (8), 3645-3649.

27. Emlyn-Jones, D., Price, G. D., and Andrews, T. J. (2003) Nitrogen-regulated hypermutator strain of *Synechococcus* sp. for use in *in vivo* artificial evolution. *Appl. Environ. Microbiol. 69* (11), 6427-6433.

28. Endo, A., Sasaki, M., Maruyama, A., and Kurusu, Y. (2006) Temperature adaptation of *Bacillus subtilis* by chromosomal *groEL* replacement. *Biosci. Biotechnol. Biochem. 70* (10), 2357-2362.

29. Shimoda, C., Itadani, A., Sugino, A., and Furusawa, M. (2006) Isolation of thermotolerant mutants by using proofreading-deficient DNA polymerase delta as an effective mutator in *Saccharomyces cerevisiae*. *Genes Genet. Syst. 81* (6), 391-397.

30. Luan, G., Cai, Z., Gong, F., Dong, H., Lin, Z., Zhang, Y., and Li, Y. (2013) Developing controllable hypermutable *Clostridium* cells through manipulating its methyl-directed mismatch repair system. *Protein Cell 4* (11), 854-862.

31. Overbeck, T. J., Welker, D. L., Hughes, J. E., Steele, J. L., and Broadbent, J. R. (2017) Transient MutS-based hypermutation system for adaptive evolution of *Lactobacillus casei* to low pH. *Appl. Environ. Microbiol. 83* (20), e01120-01117.

32. Laviña, W. A., Sakurai, S. S. M., Pontrelli, S., Putri, S. P., and Fukusaki, E. (2020) Metabolomics analysis reveals global metabolic changes in the evolved *E. coli* strain with improved growth and 1-butanol production in minimal medium. *Metabolites 10* (5), 192.

33. Kim, S. G., Noh, M. H., Lim, H. G., Jang, S., Jang, S., Koffas, M. A. G., and Jung, G. Y. (2018) Molecular parts and genetic circuits for metabolic engineering of microorganisms. *FEMS Microbiol. Lett. 365* (17).

34. Nikel, P. I., and de Lorenzo, V. (2018) *Pseudomonas putida* as a functional *chassis* for industrial biocatalysis: From native biochemistry to *trans*-metabolism. *Metab. Eng. 50*, 142-155.

35. Poblete-Castro, I., Becker, J., Dohnt, K., Martins dos Santos, V. A. P., and Wittmann, C. (2012) Industrial biotechnology of *Pseudomonas putida* and related species. *Appl. Microbiol. Biotechnol. 93* (6), 2279-2290.

36. Kivisaar, M. (2020) Narrative of a versatile and adept species *Pseudomonas putida*. *J. Med. Microbiol. 69* (3), 324-338.

37. Martínez-García, E., and de Lorenzo, V. (2019) *Pseudomonas putida* in the quest of programmable chemistry. *Curr. Opin. Biotechnol. 59*, 111-121.

38. Calero, P., Volke, D. C., Lowe, P. T., Gotfredsen, C. H., O'Hagan, D., and Nikel, P. I. (2020) A fluoride-responsive genetic circuit enables *in vivo* biofluorination in engineered *Pseudomonas putida*. *Nat. Commun. 11* (1), 5045.

39. Sánchez-Pascuala, A., Fernández-Cabezón, L., de Lorenzo, V., and Nikel, P. I. (2019) Functional implementation of a linear glycolysis for sugar catabolism in *Pseudomonas putida*. *Metab. Eng. 54*, 200-211.

40. Sánchez-Pascuala, A., de Lorenzo, V., and Nikel, P. I. (2017) Refactoring the Embden-Meyerhof-Parnas pathway as a whole of portable *GlucoBricks* for implantation of glycolytic modules in Gram-negative bacteria. *ACS Synth. Biol. 6* (5), 793-805.

41. Martínez-García, E., Aparicio, T., de Lorenzo, V., and Nikel, P. I. (2014) New transposon tools tailored for metabolic engineering of Gram-negative microbial cell factories. *Front. Bioeng. Biotechnol. 2*, 46.

42. Volke, D. C., Turlin, J., Mol, V., and Nikel, P. I. (2020) Physical decoupling of XylS/*Pm* regulatory elements and conditional proteolysis enable precise control of gene expression in *Pseudomonas putida*. *Microb. Biotechnol. 13* (1), 222-232.

43. Wirth, N. T., Kozaeva, E., and Nikel, P. I. (2020) Accelerated genome engineering of *Pseudomonas putida* by I-*Sce*I—mediated recombination and CRISPR-Cas9 counterselection. *Microb. Biotechnol. 13*, 233-249.

44. Durante-Rodríguez, G., de Lorenzo, V., and Nikel, P. I. (2018) A post-translational metabolic switch enables complete decoupling of bacterial growth from biopolymer production in engineered *Escherichia coli*. *ACS Synth. Biol. 7*, 2686-2697.

45. Kuepper, J., Otto, M., Dickler, J., Behnken, S., Magnus, J., Jäger, G., Blank, L. M., and Wierckx, N. (2020) Adaptive laboratory evolution of *Pseudomonas putida* and *Corynebacterium glutamicum* to enhance anthranilate tolerance. *Microbiology 166* (11), 1025-1037.

46. Mohamed, E. T., Werner, A. Z., Salvachúa, D., Singer, C. A., Szostkiewicz, K., Jiménez-Díaz, R. M., Eng, T., Radi, M. S., Simmons, B. A., Mukhopadhyay, A., Herrgård, M. J., Singer, S. W., Beckham, G. T., and Feist, A. M. (2020) Adaptive laboratory evolution of *Pseudomonas putida* KT2440 improves *p*-coumaric and ferulic acid catabolism and tolerance. *Metab. Eng. Commun. 11*, e00143.

47. Espeso, D. R., Dvořák, P., Aparicio, T., and de Lorenzo, V. (2020) An automated DIY framework for experimental evolution of *Pseudomonas putida*. *Microb. Biotechnol.*, DOI: 10.1111/1751-7915.13678.

48. Li, W. J., Narancic, T., Kenny, S. T., Niehoff, P. J., O'Connor, K., Blank, L. M., and Wierckx, N. (2020) Unraveling 1,4-butanediol metabolism in *Pseudomonas putida* KT2440. *Front. Microbiol. 11*, 382.

49. Li, W. J., Jayakody, L. N., Franden, M. A., Wehrmann, M., Daun, T., Hauer, B., Blank, L. M., Beckham, G. T., Klebensberger, J., and Wierckx, N. (2019) Laboratory evolution reveals the metabolic and regulatory basis of ethylene glycol metabolism by *Pseudomonas putida* KT2440. *Environ. Microbiol. 21* (10), 3669-3682.

50. Bator, I., Wittgens, A., Rosenau, F., Tiso, T., and Blank, L. M. (2019) Comparison of three xylose pathways in *Pseudomonas putida* KT2440 for the synthesis of valuable products. *Front. Bioeng. Biotechnol. 7*, 480.

51. Aparicio, T., Nyerges, A., Nagy, I., Pál, C., Martínez-García, E., and de Lorenzo, V. (2020) Mismatch repair hierarchy of *Pseudomonas putida* revealed by mutagenic ssDNA recombineering of the *pyrF* gene. *Environ. Microbiol. 22* (1), 45-58.

52. Long, H., Miller, S. F., Williams, E., and Lynch, M. (2018) Specificity of the DNA mismatch repair system (MMR) and mutagenesis bias in bacteria. *Mol. Biol. Evol. 35* (10), 2414-2421.

53. Nyerges, Á., Csörgő, B., Nagy, I., Bálint, B., Bihari, P., Lázár, V., Apjok, G., Umenhoffer, K., Bogos, B., Pósfai, G., and Pál, C. (2016) A highly precise and portable genome engineering method allows comparison of mutational effects across bacterial species. *Proc. Natl. Acad. Sci. USA 113* (9), 2502-2507.

54. Aparicio, T., Nyerges, Á., Martínez-García, E., and de Lorenzo, V. (2020) High-efficiency multi-site genomic editing (*HEMSE*) of *Pseudomonas putida* through thermoinducible ssDNA recombineering. *iScience 23* (3), 100946.

55. Benedetti, I., Nikel, P. I., and de Lorenzo, V. (2016) Data on the standardization of a cyclohexanone-responsive expression system for Gram-negative bacteria. *Data in Brief 6*, 738-744.

56. Akkaya, Ö., Pérez-Pantoja, D., Calles, B., Nikel, P. I., and de Lorenzo, V. (2018) The metabolic redox regime of *Pseudomonas putida* tunes its evolvability toward novel xenobiotic substrates. *mBio 9* (4), e01512-18.

57. Aparicio, T., de Lorenzo, V., and Martínez-García, E. (2019) Improved thermotolerance of genome-reduced *Pseudomonas putida* EM42 enables effective functioning of the P_L/*c*I857 system. *Biotechnol. J. 14* (1), e1800483.

58. Benedetti, I., de Lorenzo, V., and Nikel, P. I. (2016) Genetic programming of catalytic *Pseudomonas putida* biofilms for boosting biodegradation of haloalkanes. *Metab. Eng. 33*, 109-118.

59. Lammens, E. M., Nikel, P. I., and Lavigne, R. (2020) Exploring the synthetic biology potential of bacteriophages for engineering non-model bacteria. *Nat. Commun. 11*, 5294.

60. Martínez-García, E., Goñi-Moreno, A., Bartley, B., McLaughlin, J., Sánchez-Sampedro, L., Pascual del Pozo, H., Prieto Hernández, C., Marletta, A. S., de Lucrezia, D., Sánchez-Fernández, G., Fraile, S., and de Lorenzo, V. (2019) *SEVA 3.0*: An update of the Standard European Vector Architecture for enabling portability of genetic constructs among diverse bacterial hosts. *Nucleic Acids Res 48* (D1), D1164–D1170.

61. Villaverde, A., Benito, A., Viaplana, E., and Cubarsi, R. (1993) Fine regulation of cI857-controlled gene expression in continuous culture of recombinant *Escherichia coli* by temperature. *Appl. Environ. Microbiol. 59* (10), 3485-3487.

62. Hosokawa, K., Park, N. H., Inaoka, T., Itoh, Y., and Ochi, K. (2002) Streptomycin-resistant (*rpsL*) or rifampicin-resistant (*rpoB*) mutation in *Pseudomonas putida* KH146-2 confers enhanced tolerance to organic chemicals. *Environ. Microbiol. 4* (11), 703-712.

63. Baltz, R. H. (2014) Spontaneous and induced mutations to rifampicin, streptomycin and spectinomycin resistances in actinomycetes: Mutagenic mechanisms and applications for strain improvement. *J. Antibiot. 67* (9), 619-624.

64. Jatsenko, T., Tover, A., Tegova, R., and Kivisaar, M. (2010) Molecular characterization of Rif^R mutations in *Pseudomonas aeruginosa* and *Pseudomonas putida*. *Mutat. Res. 683* (1-2), 106-114.

65. Miskinyte, M., and Gordo, I. (2013) Increased survival of antibiotic-resistant *Escherichia coli* inside macrophages. *Antimicrob. Agents Chemother. 57* (1), 189-195.

66. Ryall, B., Eydallin, G., and Ferenci, T. (2012) Culture history and population heterogeneity as determinants of bacterial adaptation: The adaptomics of a single environmental transition. *Microbiol. Mol. Biol. Rev. 76* (3), 597-625.

67. Galhardo, R. S., Hastings, P. J., and Rosenberg, S. M. (2007) Mutation as a stress response and the regulation of evolvability. *Crit. Rev. Biochem. Mol. Biol. 42* (5), 399-435.

68. Kivisaar, M. (2010) Mechanisms of stationary-phase mutagenesis in bacteria: Mutational processes in pseudomonads. *FEMS Microbiol. Lett. 312* (1), 1-14.

69. Dvořák, P., Chrást, L., Nikel, P. I., Fedr, R., Soucek, K., Sedlacková, M., Chaloupková, R., de Lorenzo, V., Prokop, Z., and Damborský, J. (2015) Exacerbation of substrate toxicity by IPTG in *Escherichia coli* BL21(DE3) carrying a synthetic metabolic pathway. *Microb. Cell Fact. 14*, 201.

70. Silva, F., Queiroz, J. A., and Domingues, F. C. (2012) Evaluating metabolic stress and plasmid stability in plasmid DNA production by *Escherichia coli*. *Biotechnol. Adv. 30* (3), 691-708.

71. Foster, P. L. (2007) Stress-induced mutagenesis in bacteria. *Crit. Rev. Biochem. Mol. Biol. 42* (5), 373-397.

72. Węgrzyn, G., and Węgrzyn, A. (2002) Stress responses and replication of plasmids in bacterial cells. *Microb. Cell Fact. 1* (1), 2.

73. Juurik, T., Ilves, H., Teras, R., Ilmjärv, T., Tavita, K., Ukkivi, K., Teppo, A., Mikkel, K., and Kivisaar, M. (2012) Mutation frequency and spectrum of mutations vary at different chromosomal positions of *Pseudomonas putida*. *PLoS One 7* (10), e48511.

74. Long, H., Sung, W., Miller, S. F., Ackerman, M. S., Doak, T. G., and Lynch, M. (2014) Mutation rate, spectrum, topology, and context-dependency in the DNA mismatch repair-deficient *Pseudomonas fluorescens* ATCC948. *Genome Biol. Evol. 7* (1), 262-271.

75. Kivisaar, M. (2020) Mutation and recombination rates vary across bacterial chromosome. *Microorganisms 8* (1), 25.

76. Aparicio, T., Jensen, S. I., Nielsen, A. T., de Lorenzo, V., and Martínez-García, E. (2016) The Ssr protein (*T1E_1405*) from *Pseudomonas putida* DOT-T1E enables oligonucleotide-based recombineering in platform strain *P. putida* EM42. *Biotechnol. J. 11*, 1309-1319.

77. Volke, D. C., Friis, L., Wirth, N. T., Turlin, J., and Nikel, P. I. (2020) Synthetic control of plasmid replication enables target- and self-curing of vectors and expedites genome engineering of *Pseudomonas putida*. *Metab. Eng. Commun. 10*, e00126.

78. Watabe, H., Iino, T., Kaneko, T., Shibata, T., and Ando, T. (1983) A new class of site-specific endodeoxyribonucleases. Endo.*Sce*I isolated from a eukaryote, *Saccharomyces cerevisiae*. *J. Biol. Chem. 258* (8), 4663-4665.

79. Badran, A. H., and Liu, D. R. (2015) Development of potent *in vivo* mutagenesis plasmids with broad mutational spectra. *Nat. Commun. 6* (1), 8425.

80. Kurusu, Y., Narita, T., Suzuki, M., and Watanabe, T. (2000) Genetic analysis of an incomplete *mutS* gene from *Pseudomonas putida*. *J. Bacteriol. 182* (18), 5278-5279.

81. Luján, A. M., Maciá, M. D., Yang, L., Molin, S., Oliver, A., and Smania, A. M. (2011) Evolution and adaptation in *Pseudomonas aeruginosa* biofilms driven by mismatch repair system-deficient mutators. *PLoS One 6* (11), e27842.

82. Colque, C. A., Albarracín Orio, A. G., Feliziani, S., Marvig, R. L., Tobares, A. R., Johansen, H. K., Molin, S., and Smania, A. M. (2020) Hypermutator *Pseudomonas aeruginosa* exploits multiple genetic pathways to develop multidrug resistance during long-term infections in the airways of cystic fibrosis patients. *Antimicrob. Agents Chemother. 64* (5), e02142-02119.

83. Luan, G., Bao, G., Lin, Z., Li, Y., Chen, Z., Li, Y., and Cai, Z. (2015) Comparative genome analysis of a thermotolerant *Escherichia coli* obtained by genome replication engineering assisted

continuous evolution (*GREACE*) and its parent strain provides new understanding of microbial heat tolerance. *New Biotechnol. 32* (6), 732-738.

84. Nikel, P. I., Fuhrer, T., Chavarría, M., Sánchez-Pascuala, A., Sauer, U., and de Lorenzo, V. (2021) Reconfiguration of metabolic fluxes in *Pseudomonas putida* as a response to sub-lethal oxidative stress. *ISME J.*, In press, DOI: 10.1038/s41396-41020-00884-41399.

85. Shibai, A., Takahashi, Y., Ishizawa, Y., Motooka, D., Nakamura, S., Ying, B. W., and Tsuru, S. (2017) Mutation accumulation under UV radiation in *Escherichia coli*. *Sci. Rep. 7* (1), 14531.

86. Castañeda-García, A., Prieto, A. I., Rodríguez-Beltrán, J., Alonso, N., Cantillon, D., Costas, C., Pérez-Lago, L., Zegeye, E. D., Herranz, M., Plociński, P., Tonjum, T., García de Viedma, D., Paget, M., Waddell, S. J., Rojas, A. M., Doherty, A. J., and Blázquez, J. (2017) A non-canonical mismatch repair pathway in prokaryotes. *Nat. Commun. 8*, 14246.

87. Groothuizen, F. S., and Sixma, T. K. (2016) The conserved molecular machinery in DNA mismatch repair enzyme structures. *DNA Repair 38*, 14-23.

88. Jacquelín, D. K., Filiberti, A., Argaraña, C. E., and Barra, J. L. (2005) *Pseudomonas aeruginosa* MutL protein functions in *Escherichia coli*. *Biochem. J. 388* (3), 879-887.

89. Nyerges, Á., Csorgő, B., Nagy, I., Latinovics, D., Szamecz, B., Pósfai, G., and Pál, C. (2014) Conditional DNA repair mutants enable highly precise genome engineering. *Nucleic Acids Res. 42* (8), e62.

90. Green, M. R., and Sambrook, J., *Molecular cloning: a laboratory manual*. 4th ed.; Cold Spring Harbor Laboratory Press: Cold Spring Harbor, NY, 2012.

91. Nour-Eldin, H. H., Geu-Flores, F., and Halkier, B. A. (2010) *USER* cloning and *USER* fusion: The ideal cloning techniques for small and big laboratories. *Methods Mol. Biol. 643*, 185-200.

92. Choi, K. H., Kumar, A., and Schweizer, H. P. (2006) A 10-min method for preparation of highly electrocompetent *Pseudomonas aeruginosa* cells: Application for DNA fragment transfer between chromosomes and plasmid transformation. *J. Microbiol. Methods 64*, 391-397.

93. Li, H., and Durbin, R. (2009) Fast and accurate short read alignment with Burrows-Wheeler transform. *Bioinformatics 25* (14), 1754-1760.

94. Danecek, P., Bonfield, J. K., Liddle, J., Marshall, J., Ohan, V., Pollard, M. O., Whitwham, A., Keane, T., McCarthy, S. A., Davies, R. M., and Li, H. (2021) Twelve years of SAMtools and BCFtools. *GigaScience 10* (2).

95. Wang, K., Li, M., and Hakonarson, H. (2010) *ANNOVAR*: Functional annotation of genetic variants from high-throughput sequencing data. *Nucleic Acids Res. 38* (16), e164.

96. Meselson, M., and Yuan, R. (1968) DNA restriction enzyme from *E. coli*. *Nature 217* (5134), 1110-1114.

97. Bagdasarian, M., Lurz, R., Rückert, B., Franklin, F. C. H., Bagdasarian, M. M., Frey, J., and Timmis, K. N. (1981) Specific purpose plasmid cloning vectors. II. Broad host range, high copy number, RSF1010-derived vectors, and a host-vector system for gene cloning in *Pseudomonas*. *Gene 16* (1-3), 237-247.

98. Martínez-García, E., Nikel, P. I., Aparicio, T., and de Lorenzo, V. (2014) *Pseudomonas* 2.0: Genetic upgrading of *P. putida* KT2440 as an enhanced host for heterologous gene expression. *Microb. Cell Fact. 13* (1), 159.

99. Silva-Rocha, R., Martínez-García, E., Calles, B., Chavarría, M., Arce-Rodríguez, A., de las Heras, A., Páez-Espino, A. D., Durante-Rodríguez, G., Kim, J., Nikel, P. I., Platero, R., and de Lorenzo, V. (2013) The Standard European Vector Architecture (SEVA): A coherent platform for the analysis and deployment of complex prokaryotic phenotypes. *Nucleic Acids Res. 41* (D1), D666-D675.

Table 1. Bacterial strains and plasmids used in this work.

Bacterial strain	Relevant characteristics[a]	Reference
Escherichia coli		
DH5α	Cloning host; F⁻ λ⁻ *endA1 glnX44*(AS) *thiE1 recA1 relA1 spoT1 gyrA96*(Nal^R) *rfbC1 deoR nupG Φ80(lacZΔM15) Δ(argF-lac)U169 hsdR17 rK7*(r_K^- m^+_K)	Meselson and Yuan[96]
Pseudomonas putida		
KT2440	Wild-type strain; derivative of *P. putida* mt-2 cured of the TOL plasmid pWW0	Bagdasarian *et al.*[97]
EM42	Derivative of *P. putida* KT2440; Δprophage1 Δprophage2 Δprophage3 Δprophage4 ΔTn*7* Δ*endA-1* Δ*endA-2* Δ*hsdRMS* Δflagellum ΔTn*4652*	Martínez-García *et al*.[98]
pyrF HM	Derivative of *P. putida* EM42; *pyrF*^{Lys55STOP} (A163T)	Aparicio *et al.*[76]
Plasmids		
pSEVA2311	Standard cyclohexanone-responsive expression vector; Km^R; *oriV*(pBBR1), *chnR*/P_{chnB}	Benedetti *et al.*[55]
pSEVA2514	Standard thermo-inducible expression vector; Km^R; *oriV*(RSF1010), *cI857*/P_L	Aparicio *et al.*[57]
pSEVA2514-*rec2*-*mutL*$_{E36K}^{PP}$	Derivative of vector pSEVA2514 carrying the *rec2* recombinase and the dominant-negative mutator *mutL*^{E36K} allele from *P. putida*	Aparicio *et al*.[51]
pQURE6·L	Conditionally-replicating vector; derivative of vector pJBSD1 carrying XylS/*Pm*→*I-SceI* and P_{14g}→*mCherry*; Gm^R	Volke *et al.*[77]
pS2311SG	Derivative of vector pSEVA2311 with an engineered *I-SceI* recognition site for easy vector curing and P_{EM7}→*msfGFP*	This work
pS2514SG	Derivative of vector pSEVA2514 with an engineered *I-SceI* recognition site for easy vector curing and P_{EM7}→*msfGFP*	This work
pS2311M	Derivative of vector pSEVA2311 carrying the dominant-negative mutator *mutL*^{E36K} allele from *P. putida*	This work
pS2514M	Derivative of vector pSEVA2514 carrying the dominant-negative mutator *mutL*^{E36K} allele from *P. putida*	This work

pS2311SGM	Derivative of vector pS2311SG carrying the dominant-negative mutator *mutL*^{E36K} allele from *P. putida*	This work
pS2514SGM	Derivative of vector pS2514SG carrying the dominant-negative mutator *mutL*^{E36K} allele from *P. putida*	This work

[a] Antibiotic markers: Km, kanamycin; Gm, gentamicin; Nal, nalidixic acid.

FIGURE LEGENDS

Figure 1. Broad-host-range mutator devices to conditionally increase mutation rates. (a) The bacterial DNA mismatch repair (MMR) system recognizes and fixes mutations that arise during DNA replication and recombination. MutS recognizes genomic DNA mismatches and recruits MutL. The MutL/MutS complex activates the MutH endonuclease, which cleaves the newly synthesized, unmethylated daughter strand at the nearest hemimethylated d(GATC) site, and thereby marks it for a removal and a repair–synthesis process that involves a variety of other proteins. Overexpression of the dominant-negative mutator allele *mutL*^{E32K} from *E. coli* increases mutation rates[25]. **(b)** Structure of the two mutator devices used in this work. Plasmids pS2514M and pS2311M, based on the *Standard European Vector Architecture*[99], were designed for thermo-inducible or cyclohexanone-inducible expression of the mutator allele *mutL*^{E36K} from *P. putida*, respectively. Functional elements in the plasmids not drawn to scale; *Km*^{R}, kanamycin-resistance marker. **(c)** Two strategies for tampering with the MMR system of *P. putida*. When using plasmid pS2514M, the temperature-sensitive repressor *c*I857 is constitutively produced at 28-32°C and specifically binds to the P_L promoter, mediating transcriptional repression of the gene cloned downstream (i.e. *mutL*^{E36K}). By shifting the temperature above 37°C (e.g. 40°C), the expression of *mutL*^{E36K} can take place due to denaturation of *c*I857. When using plasmid pS2311M, the ChnR transcriptional regulator is constitutively synthetized and binds to the P_{chnB} promoter in the presence of its inducer (cyclohexanone), thus causing the expression of the gene cloned downstream (i.e. *mutL*^{E36K}).

Figure 2. Experimental setup for evolution of *P. putida* strains carrying mutator plasmids. Control (ctrl.) strains (i.e. *P. putida* KT2440/pSEVA2311 and KT2440/pSEVA2514, bearing empty vectors) and conditional-mutator strains (i.e. *P. putida* KT2440/pS2311M and KT2440/pS2514M) were incubated in shaken-flask cultures in a non-selective medium (i.e. M9 minimal medium containing 20 mM glucose). After 5 h, when cultures reached an optical density at 600 nm (OD_{600}) = 0.3, the expression systems were induced either thermally (incubating the flasks in a water bath) or chemically (adding liquid cyclohexanone to the medium). The cultures were re-incubated at 30°C with shaking and the process was stopped after 1.5 h (early exponential phase, OD_{600} = 0.6), 2 h (mid-exponential phase, OD_{600} = 1) or 24 h (stationary phase). In the case of cultures of *P. putida* KT2440 carrying either vector pSEVA2311 or plasmid pS2311M, the biomass was washed twice with phosphate buffer to remove any traces of cyclohexanone. Several aliquots were plated onto a selective solid medium [e.g. LB agar supplemented with streptomycin (Str) or rifampicin (Rif)] to assess the appearance of mutants in the bacterial population [e.g. rifampicin-(Rif^R) or streptomycin-resistant (Str^R) mutants]. The total number of viable cells in the bacterial cultures was estimated by plating dilutions of the cultures on non-selective solid medium (e.g. LB agar). *CFU*, colony-forming unit.

Figure 3. Evolution of antibiotic resistance in *P. putida* using conditional mutator devices. *P. putida* strains carrying the systems inducible by cyclohexanone **(a)** and temperature shifts **(b)** were evolved by following the mutagenesis protocol described in **Fig. 2**. Culture aliquots were plated onto selective medium [i.e. LB agar supplemented with 100 μg mL^{-1} streptomycin (Str) or 50 μg mL^{-1} rifampicin (Rif)] to determine the appearance of Rif- (Rif^R) or Str-resistant (Str^R) mutants. The total number of viable cells was estimated by plating dilutions of each of the cultures onto LB agar plates. Two technical replicates and several dilutions for replicate were performed for each bacterial strain and per each selective culture condition. Columns represent mean values of mutation frequencies (MF, expressed as the number of mutant cells per 1×10^9 viable *P. putida* cells) from at least two independent experiments ± standard deviation. *Relative mutation frequencies* were obtained by comparing the mutation frequency of the conditional mutator strain with the respective control (ctrl.) strain in the same experimental setup (i.e. expressed as fold-change).

Figure 4. Reversion of a synthetic uracil auxotrophy in *P. putida* using mutator devices. (a) *P. putida pyrF* HM, carrying the *pyrF*^{Lys55STOP} allele that confers uracil auxotrophy (Ura$^-$ phenotype), was transformed with the two conditional mutator systems (i.e. inducible by cyclohexanone or temperature shifts) or the corresponding control (ctrl.) vectors, and evolved by following the mutagenesis protocol described in **Fig. 2**. Several aliquots of these bacterial cultures were plated on selective solid medium (i.e. M9 minimal medium containing glucose as the only carbon source) to estimate the appearance of uracil prototrophic mutants (Ura$^+$) in the population. The total number of viable cells was estimated by plating dilutions of the same cultures onto M9 minimal medium plates supplemented with 20 mM glucose and 20 μg mL^{-1} uracil. Two technical replicates and several dilutions for replicate were performed for each bacterial strain and per each selective culture condition. Columns represent mean values of mutation frequencies (expressed as the number of mutant cells per 1×10^9 viable *P. putida pyrF* HM cells) from at least two independent experiments ± standard deviation. **(b)** Mutations found in the *pyrF* gene (*PP_1815*) in the Ura$^+$ mutants isolated from two independent experiments. A total of eight Ura$^+$ mutants for each mutator/control strain were analyzed. **(c)** Frequency of mutation occurrence in a control (ctrl.) strain and in the strain carrying the conditional mutator devices. Stop codons are indicated with the abbreviation *STOP*.

Figure 5. Design and implementation of a new generation of plasmid-based, easy-to-cure mutator devices for Gram-negative bacteria. (a) Plasmids pS2311SG, pS2514SG, pS2311SGM and pS2514SGM, derivatives of vectors pSEVA2311, pSEVA2514, pS2311M and pS2514M, respectively, were engineered with a I-*Sce*I recognition site (indicated at the bottom of the figure) to render them compatible with the plasmid curing system based on targeted degradation mediated by the I-*Sce*I endonuclease[77]. These conditional mutator plasmids also carry a synthetic module for the constitutive expression of *msfGFP* (i.e. P_{EM7}→*msfGFP*) that facilitate the selection of green fluorescent clones by examination of colonies under blue light. Functional elements in the plasmids not drawn to scale; Km^R, kanamycin-resistance marker; *MCS*, standard multiple cloning site. **(b)** Mutation spectra caused by the mutator devices classified in functional categories. Control strains [i.e. *P. putida* KT2440/pS2514SG (TC) and KT2440/pS2311SG (CC)] and the conditional mutator strains [i.e. *P. putida* KT2440/pS2514SGM (TM) and KT2440/pS2311SGM (CM)] were incubated in shaken-flasks in a non-selective culture medium. After 5 h (OD_{600} = 0.3), expression systems were induced thermally (in a water bath at 40°C for 15 min) or chemically (addition of 1 mM cyclohexanone). All cultures (induced and non-induced) were re-incubated at 30°C until reaching an OD_{600} = 0.6. Several dilutions of the cultures were plated on LB agar for isolation of individual colonies. After curing off the mutator and control (i.e. empty) plasmids from the respective clones, genomic DNA was isolated, sequenced and the readings assembled. The emergence of transition (A:T→G:C; G:C→A:T), transversion (A:T→T:A; G:C→T:A; A:T→C:G; G:C→C:G) and small insertion-deletion (InDel) events (< 50 bp) mutations was analyzed in the individual strains. Clones 1-5 and clones 6-10 were obtained from induced and non-induced cultures, respectively.

Figure 6. Evolution of a dual antibiotic resistance in *P. putida* using conditional mutator devices. The control strain *P. putida* KT2440/pSEVA2311SG and the conditional-mutator strain *P. putida* KT2440/pS2311SGM were incubated in shaken-flask cultures in a non-selective medium (i.e. M9 minimal medium containing 20 mM glucose) for 24 h (stationary phase). Several aliquots cultures were plated onto a selective solid medium [i.e. LB agar supplemented with 50 μg mL^{-1} kanamycin (Km), 50 μg mL^{-1} rifampicin (Rif) and 100 μg mL^{-1} streptomycin (Str)] to assess the appearance of mutants [e.g. rifampicin-(Rif^R) and streptomycin-resistant (Str^R) mutants]. The total number of viable cells in the bacterial cultures was estimated by plating dilutions of the cultures on non-selective solid medium (e.g. LB agar supplemented with Km). Two replicates and several dilutions for replicate were performed for each bacterial strain and per each selective culture condition. **(a)** Representative Petri dishes from these experiments were photographed for the sake of a rough comparison of the number of colonies observed for each culture under selective culture conditions. **(b)** Quantification of mutation frequencies. Columns represent mean values of the actual mutation frequencies (expressed as the number of mutant cells per 1×10^9 viable *P. putida* cells) from two independent experiments ± standard deviation.

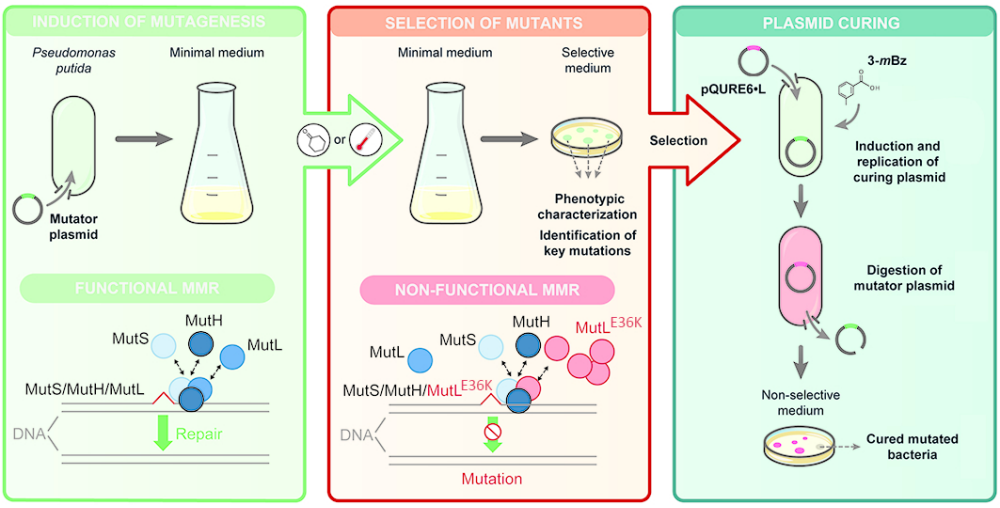
INDUCTION OF MUTAGENESIS
Pseudomonas putida
Minimal medium
Mutator plasmid
FUNCTIONAL MMR
MutH
MutS
MutL
MutS/MutH/MutL
DNA
Repair
or
SELECTION OF MUTANTS
Minimal medium
Selective medium
Phenotypic characterization
Identification of key mutations
NON-FUNCTIONAL MMR
MutH
MutS
MutL
MutL E36K
MutS/MutH/MutL E36K
DNA
Mutation
Selection
PLASMID CURING
pQURE6•L
3-mBz
Induction and replication of curing plasmid
Digestion of mutator plasmid
Non-selective medium
Cured mutated bacteria

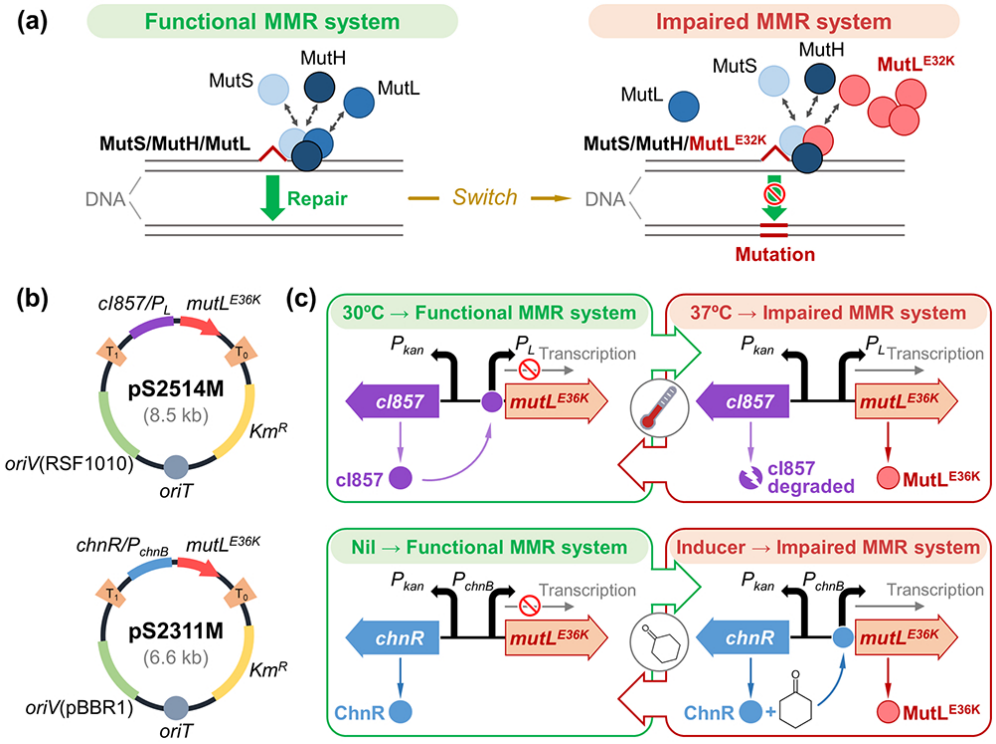
(a)
Functional MMR system
Impaired MMR system
MutS
MutH
MutL
MutS/MutH/MutL
DNA
Repair
Switch
MutL E32K
MutS/MutH/MutL E32K
Mutation
(b)
cI857/P_L
mutL E36K
pS2514M
(8.5 kb)
Km R
oriV(RSF1010)
oriT
chnR/P_chnB
pS2311M
(6.6 kb)
oriV(pBBR1)
(c)
30°C → Functional MMR system
37°C → Impaired MMR system
P_kan
P_L
Transcription
cI857
cI857 degraded
MutL E36K
Nil → Functional MMR system
Inducer → Impaired MMR system
P_chnB
chnR
ChnR

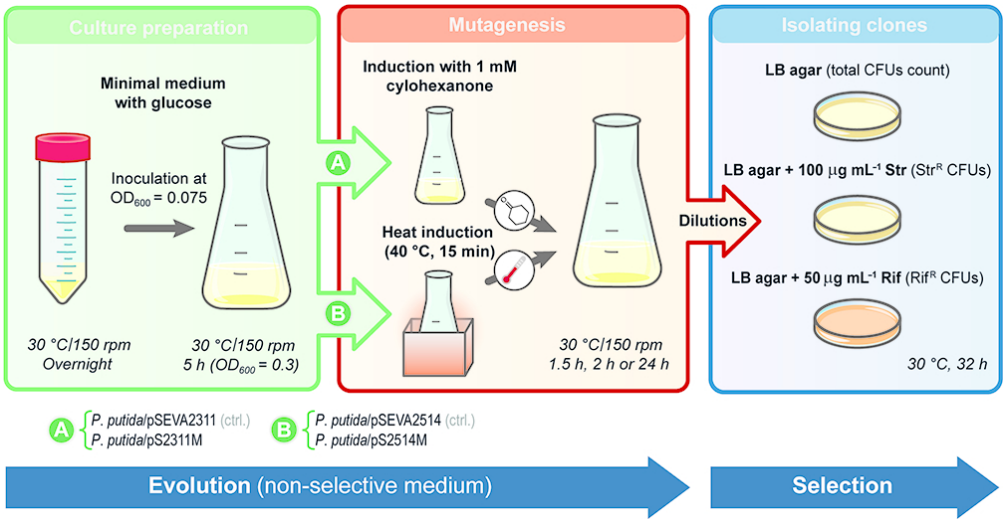
Culture preparation
Minimal medium with glucose
Inoculation at OD_{600} = 0.075
30 °C/150 rpm Overnight
30 °C/150 rpm 5 h (OD_{600} = 0.3)
Mutagenesis
Induction with 1 mM cylohexanone
Heat induction (40 °C, 15 min)
30 °C/150 rpm 1.5 h, 2 h or 24 h
Isolating clones
LB agar (total CFUs count)
LB agar + 100 μg mL-1 Str (StrR CFUs)
LB agar + 50 μg mL-1 Rif (RifR CFUs)
30 °C, 32 h
Dilutions
A P. putida/pSEVA2311 (ctrl.) P. putida/pS2311M
B P. putida/pSEVA2514 (ctrl.) P. putida/pS2514M
Evolution (non-selective medium)
Selection

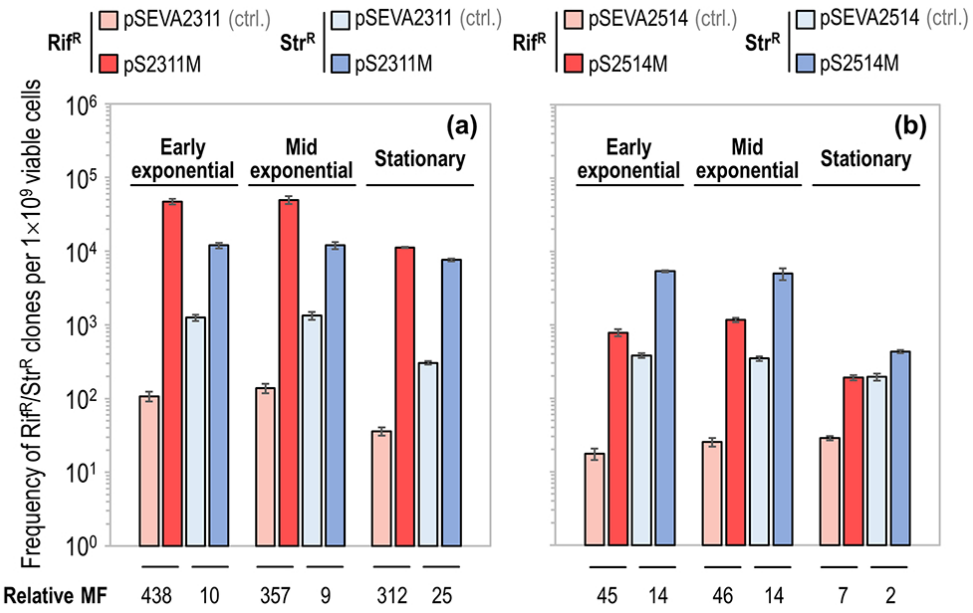
Rif^R
pSEVA2311 (ctrl.)
pS2311M
Str^R
pSEVA2311 (ctrl.)
pS2311M
Rif^R
pSEVA2514 (ctrl.)
pS2514M
Str^R
pSEVA2514 (ctrl.)
pS2514M
Frequency of Rif^R/Str^R clones per 1×10^9 viable cells
10^6
10^5
10^4
10^3
10^2
10^1
10^0
(a)
(b)
Early exponential
Mid exponential
Stationary
Relative MF
438 10 357 9 312 25
45 14 46 14 7 2

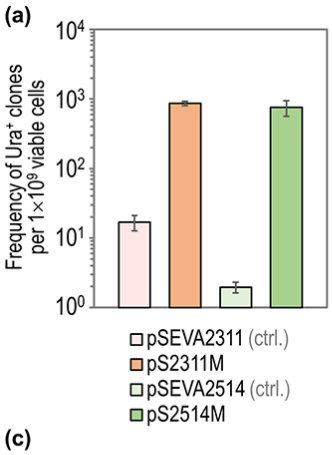

(c)

DNA change	Amino acid change	Ocurrence (%)	
		Ctrl.	+ Mutator device
163(T→G)	*STOP*55Glu	60	0
164(A→T)	*STOP*55Leu	10	0
164(A→G)	*STOP*55Trp	0	56
163(T→C)	*STOP*55Gln	10	44
164(A→C)	*STOP*55Ser	20	0

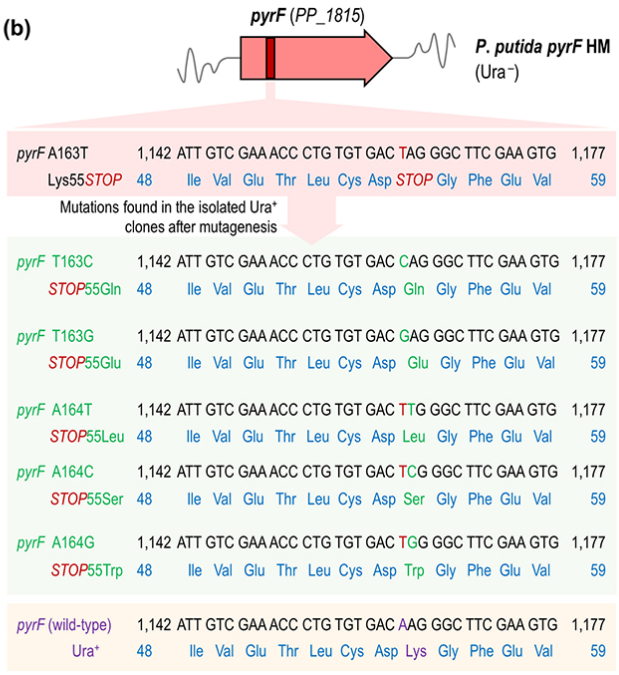

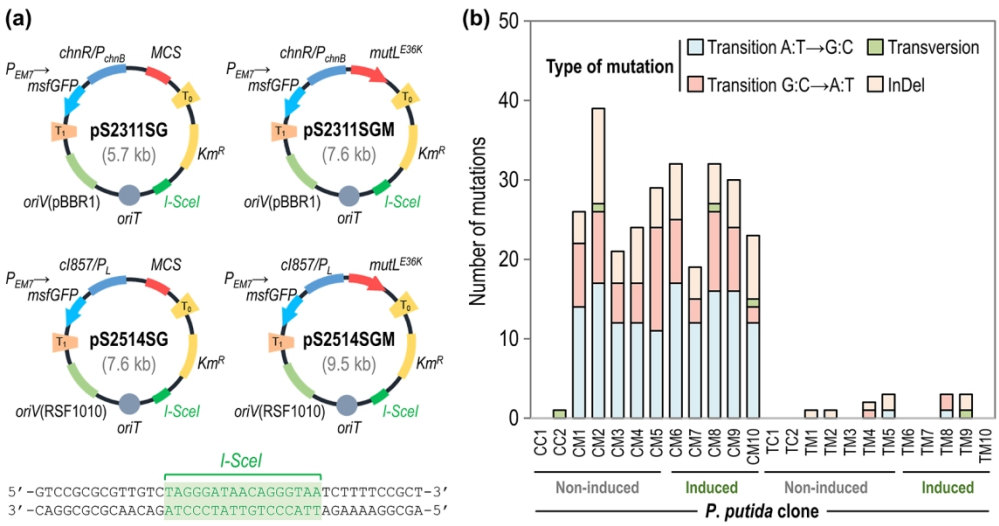
(a)
chnR/P_chnB
MCS
P_EM7
msfGFP
pS2311SG
(5.7 kb)
Km^R
oriV(pBBR1)
I-SceI
oriT
mutL^E36K
pS2311SGM
(7.6 kb)
cI857/P_L
pS2514SG
(7.6 kb)
oriV(RSF1010)
pS2514SGM
(9.5 kb)
I-SceI
5′-GTCCGCGCGTTGTCTAGGGATAACAGGGTAATCTTTTCCGCT-3′
3′-CAGGCGCGCAACAGATCCCTATTGTCCCATTAGAAAAGGCGA-5′
(b)
Type of mutation
Transition A:T→G:C
Transversion
Transition G:C→A:T
InDel
Number of mutations
0
10
20
30
40
50
CC1
CC2
CM1
CM2
CM3
CM4
CM5
CM6
CM7
CM8
CM9
CM10
TC1
TC2
TM1
TM2
TM3
TM4
TM5
TM6
TM7
TM8
TM9
TM10
Non-induced
Induced
Non-induced
Induced
P. putida clone

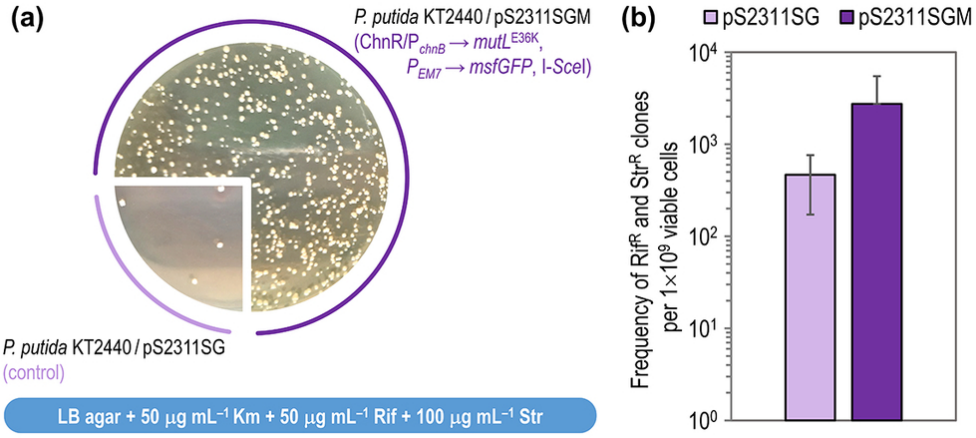

84x39mm (300 x 300 DPI)